VALIDATED AXIAL RESIDUAL STRESS PROFILES FOR FRACTURE ASSESSMENTS OF AUSTENITIC STAINLESS STEEL PIPE GIRTH WELDS

Mr P J Bouchard
British Energy Generation Ltd.
Barnett Way, Barnwood
Gloucester GL4 3RS
UK

Tel: 44 (0)1452 653160
Fax: 44 (0)1452 653025
email: john.bouchard@british-energy.com

Dr R A W Bradford
British Energy Generation Ltd.
Barnett Way, Barnwood
Gloucester GL4 3RS
UK

Tel: 44 (0)1452 653237
Fax: 44 (0)1452 653896
email: rick.bradford@british-energy.com

ABSTRACT

Defect assessments for plant components are increasingly used by many industries to develop and optimise new designs, or to support management of existing engineering plant. Such fracture assessments can be highly sensitive to weld residual stress profiles assumed in the calculations. This is illustrated for typical stainless steel pipe girth welds, where there is a lack of consensus in structural integrity procedures and published compendia about what axial residual stress profiles to use. A general prescription for detailed as-welded residual stress distributions in stainless steel pipe butt welds of arbitrary diameter and thickness has been published recently. This prescription, based on finite element studies, is critically examined by comparing the predicted profiles with an array of diverse weld residual stress surements in pipe welds 16-65mm thick. An improved ıormulation is proposed that provides a reasonably accurate and generally conservative detailed description of the measured axial residual stresses. The new approximation is simple to evaluate and gives profiles that are self-equilibrating through the section. It is therefore ideally suited for use in fracture assessments.

NOMENCLATURE

A	weld metal cross-section area, mm^2
I	welding electrical current, A
N	number of weld passes
q	weld arc power, =IV, W
Q	weld pass heat input, KJ/mm
$\tilde{Q}$	weld pass heat input per unit thickness, KJ/mm^2
R	mean pipe radius, mm
t	pipe thickness, mm
v	weld arc advance rate, mm/s
V	weld pass closed circuit electrical voltage, V
x	distance through thickness from inner radius, mm
α	heat input sinusoid correlation factor
β	heat input linear bending correlation factor
σ_{axial}	axial residual stress, MPa
σ_y	material yield stress, MPa
BRSL	block removal, splitting and layering
CL	weld centre-line
DH	deep hole residual stress measurement
FCP	first weld cap pass
HAZ	heat affected zone
LCP	last weld cap pass
ND	neutron diffraction stress measurement
PS	proof stress
SH	surface centre-hole residual stress measurement

INTRODUCTION

Tensile residual stress in engineering structures generally has an adverse effect on life. Residual stress alone can initiate cracking, even before a component enters service. When combined with stresses due to service loads, tensile residual stress reduces crack initiation life accelerates growth rates of pre-existing or service-induced defects, and increases the susceptibility of structures to catastrophic failure by fracture. Conversely, compressive residual stress can improve structural performance.

The importance of residual stress to industry depends on the engineering application and design philosophy employed. For example, knowledge of residual stresses is not usually required for steel components designed to 'traditional' construction codes, whereas damage tolerance assessments for safety-related plant need a thorough understanding of the residual stress field and how it affects component life. Integrity assessments of the latter kind are increasingly being used by many industries to develop and optimise new designs, or to support management of existing engineering plant.

The influence of residual stress on the fracture behaviour of a structure depends on the type of loading and the level of plasticity induced. Under predominately elastic conditions, residual stress significantly reduces the load carrying capacity. Conversely, the impact of residual stress on integrity is small when plasticity is widespread owing to mechanical stress-relief effects. Defect assessment procedures, such as R6 (British Energy, 2001), have been developed and validated to assess the full brittle-ductile range of fracture behaviour in defective engineering components. R6 accounts for the interaction of primary and secondary loads, including residual ss, at various levels of sophistication, depending on the accuracy of atment required. Thus it can allow for the reduced influence of residual stress on fracture behaviour as plasticity becomes more widespread.

Accurate defect assessments require a good description of the through-wall residual stress field in the component. However, reliable characterisation of residual stresses at non-stress-relieved welds is notoriously difficult. Simple estimates, denoted Level 1 in R6, enable an initial conservative assessment of a defect to be made by assuming a uniformly distributed tensile residual stress equal in magnitude to the mean material yield strength. A more realistic characterisation approach (Level 2) is to define a conservative through-wall residual stress profile for the class of weld, based on structural integrity procedure recommendations or published compendia. The third approach (Level 3) is the most involved but provides details of the magnitude and spatial distribution of weld residual stress. It requires non-linear analytical modelling of the processes responsible for inducing the residual stress coupled with experimental measurements. The choice of approach depends on the nature of the residual stress field and the engineering context.

The Level 2 approach is most commonly used for defect ssments, as this provides a conservative residual stress description minimum effort. However, for some classes of weld, there is a lack of consensus between different structural integrity procedures and published compendia about what residual stress profiles to use. This paper illustrates the range of residual stress profiles recommended for assessments of defects in non-stress relieved pipe girth welds. In particular, the new prescription of Bradford (2000) for detailed through-wall residual stress profiles in stainless steel cylindrical butt welds is examined. This generic prescription is based on a consistent set of finite element simulations for a comprehensive combination of geometric parameters and weld heat inputs. The first objective of this paper is to demonstrate the sensitivity of a standard R6 defect assessment to recommended residual stress profile assumptions, using the example of a stainless steel pipe girth weld. The second objective is to examine the performance of the Bradford prescription for girth welds by comparing the predicted profiles for axial residual stresses with an array of diverse measurements on pipes 16 - 65mm thick. The third objective is to propose an improved predictive formulation for fracture assessments based on the measured data.

WELD RESIDUAL STRESS PROFILES

Fusion welding processes for structural applications involve the progressive melting of parent material and usually the deposition of additional molten filler material. Residual stresses in the structure are induced mainly by thermal contraction of the molten material. However, adjacent material in the heat affected zone (HAZ), which does not reach melting point, experiences very high thermal stresses that are sufficient to cause cyclic yielding. In multi-pass welds, later runs heat earlier passes allowing some stress relaxation to occur, and impose incremental contraction loads on cooling. These effects produce a complex pattern of local strain and residual stress throughout the weld and surrounding HAZ material. The stiffness of the structure and imposed restraint conditions define the global response of the joint to the welding process, and therefore control the general characteristics of the final residual stress field. Thus, there are various factors that influence the magnitude and variation of weld residual stresses in structural components:

i) the weld geometry (including the effect of structural restraint);

ii) the weld procedure (heat input, number of passes, deposition sequence etc.); and

iii) the weld and parent material properties.

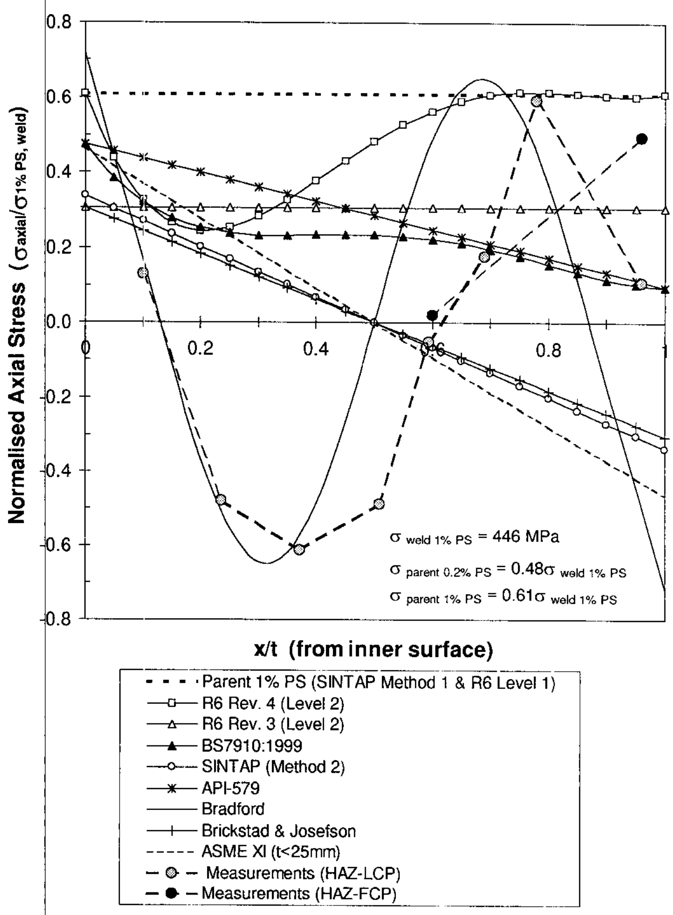

Figure 1: Comparison of axial residual stress profiles for a pipe girth weld (t=19.6mm, R/t=10.5, Q=1.4 KJ/mm)

It is sometimes possible to de-convolute through-wall weld residual stress profiles into component parts classifiable as short-, medium- and long-range (British Energy, 2001) depending on the length scale away from the weld over which the residual stress dies away. Long-range residual stresses have a membrane or through-wall bending character and exhibit significant elastic-follow-up. They usually develop from global or imposed boundary restraint that commonly arises during the fabrication of complex multi-component structures. Medium range residual stresses tend to be membrane and through-wall bending components of stress with low elastic follow-up and are usually induced by the self-restraint of the structure to weld shrinkage parameters, in the absence of external boundary conditions. Short-range residual stresses are generally completely self-balancing (membrane and bending) over a weld cross-section and are associated with non-uniform plastic strains induced by the incremental response of the structure to multiple passes and by local weld bead deposition sequence effects.

The detailed spatial variation of residual stress (long + medium + short range) near component surfaces is important for assessing crack initiation life and short-crack growth. In contrast, it is the underlying through-wall residual stress profile (long + medium range) that influences final fracture from defects sufficiently large to threaten structural integrity. However, when defects are small compared with the wavelength of the short-range stresses, and when it is not admissible to claim crack growth arising from stable ductile tearing, the total residual stress profile (combined long, medium, and short-range components) has to be assumed for practical defect assessments.

Combined medium and short-range weld residual stress profiles for fracture assessments can be found in structural integrity assessment procedures and compendia, for example (British Energy, 2000, 2001), (SINTAP, 1999), (API, 2000), (BSi, 2000), (ASME, 1986), (Bate, 2000), (Brickstad, 1998), (Bradford, 2000). Figure 1 illustrates some of the alternative recommended axial through-wall residual stress profiles available for a typical stainless steel pipe girth weld. A wide variation in the shapes and magnitudes of the profiles is evident. For example at the outer surface, stresses range from +60% to -70% of the weld 1% proof stress. This situation has arisen because bounding methodologies have been applied by various workers to different sub-sets of finite element and/or measured residual stress data covering a wide range of geometry, material and weld procedure parameters. As described earlier, residual stresses in welds depend on complex interacting factors. These are difficult to simulate consistently using finite element methods. Defining reliable weld residual stress profiles from measurements is also problematic because of the complex local and global spatial distributions of stress, the innate variability of residual stress fields (even in welds fabricated to identical procedures) and because of the limitations of the measurement techniques themselves. As more numeric and measured data are accumulated, it seems inevitable that a 'conservative' line bounding all the data will tend to approach uniform yield magnitude. For example Revision 4 of the R6 defect assessment procedure (British Energy, 2001) recommends a more conservative axial residual stress profile than R6 Revision 3 (British Energy, 2000), as illustrated in Fig. 1.

FRACTURE ASSESSMENT EXAMPLE

The significance of the assumed residual stress distribution in fracture assessments has been examined using Revision 4 of the R6 defect assessment procedure (British Energy, 2001).

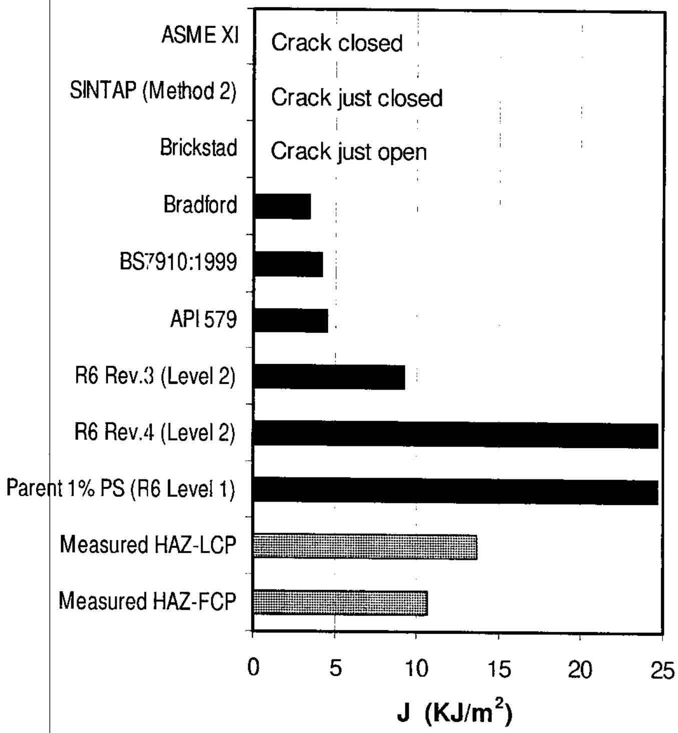

Figure 2: R6 estimated *J*-integral results using alternative residual stress profiles for a 5mm deep, 50mm long circumferential external crack in a t=19.6mm girth weld.

A typical defect, of depth 5mm from the outer surface and surface length 50mm, was assumed to be present along the fusion boundary of a 19.6mm thick, 216mm outer radius, pipe girth weld. A design pressure of 14.1 MPa plus an axial membrane stress of 40 MPa was assumed to apply. The 40 MPa axial stress represents a typical value that might be present from pipe-work loads. The effect of each of the different residual stress profiles shown in Fig. 1 was examined in turn.

The fracture assessments employed the R6 Option 1 failure assessment diagram using the simple ρ plasticity correction for secondary stresses based on elastic stress intensity factor calculations. The limit load was pressure (hoop stress) dominated, because of the small crack size, giving a constant value of the L_r parameter (representing proximity to plastic yielding) equal to 0.67 for a mean 0.2% proof stress of 212 MPa. Note that at this value of L_r nearly elastic conditions prevailed in the fracture assessments making them more sensitive to residual stress.

The crack tip J-integral was estimated using the R6 approach via the following expression:

$$J = \frac{J_e}{\left[f(L_r) - \rho\right]^2} \qquad (1)$$

where the elastic J-integral, J_e, is derived from the total linear elastic stress intensity factor using a Young's modulus of 195.6 GPa and Poisson's ratio of 0.29, and $f(L_r)$ defines the R6 failure assessment curve. This approach was used to evaluate the R6 based J-integral values presented in Fig. 2 for the assumed outer surface breaking defect, 5mm deep by 50mm long.

Figure 2 vividly demonstrates the large effect residual stress profile assumptions have on fracture assessments. The results based on best-estimate measured profiles indicate the non-conservatism or conservatism of the profiles for the specific defect examined. Because of the varying nature of most of the profiles, different sizes of defect and pipe loading conditions would give a quite different set of results. Therefore no overall conclusion about the merits of particular prescriptions can be drawn, apart from the yield stress assumption that is always expected to be conservative. What can be seen from Fig. 1 is that only the Bradford prescription gives a profile that roughly matches the measured stresses, but this gives a non-conservative *J* result for the case considered.

	Weld C	SP19	OU20	SP37	S5
t (mm)	15.9	19.6	20	37	65
[illegible]	25	10.5	3.8	5.3	2.8
Weld type	SAW *	MMA	MMA	MMA	MMA
No. Passes, N	4 *	16	13	26	# - 44
Q (KJ/mm)	2.2	1.4	1.8	2.2	1.0 - 2.4
$\tilde{Q}$ (KJ/mm^2)	136	73	91	59	15 – 37
Weld Material	316L	316L	316L	316L	316L
$\sigma_{1\%\ PS}$ (MPa)	476	446	446	446	446
Parent material	316L	316H	316L	316H	316H
$\sigma_{0.2\%\ PS}$ (MPa)	296	212	264	287	287
$\sigma_{1\%\ PS}$ (MPa)	338	272	308	328	328
$\sigma_{10\%\ PS}$ (MPa)	480	-	-	461	461
Residual Stress Measurements	ND, SH, BRSL	ND, SH, DH	ND	DH	DH, SH

ND = Neutron Diffraction, DH = Deep Hole, SH = Surface Hole
BRSL = Block Removal, Splitting and Layering.
* Outer V passes of double V-prep. Weld
\# Number of passes unknown for low heat input S5 welds

Table 1: Details of Girth Welds and Stress Measurements

GIRTH WELD MEASURED RESIDUAL STRESSES

A programme of residual stress measurements has been carried out on the pipe girth welds listed in Table 1, for the purpose of validating finite element residual stress simulations. The pipes were made from various grades of AISI type 316 austenitic stainless steel (note that pipe SP19 was made from solution heat-treated material). Type 316L weld electrodes were used in all cases. Four of the pipe types had a single external J-preparation groove, filled using a manual metal arc (MMA) technique. One pipe (Weld C) had a double-V groove with a small inner-V filled by MMA and the larger outer-V filled by high heat input submerged arc weld passes (SAW). A total of three types of S5 weld mock-ups (see Table 1) were made using different MMA weld heat inputs. Heat input values, Q, for Weld C and some of the S5 mock-ups were measured during fabrication. Average heat inputs for the other welds were calculated using the following expression:

$$Q = \frac{q}{v} = 0.071\frac{A}{N} \quad \text{for } Q \leq 1.8 \text{ KJ/mm} \qquad (2)$$

where q is the weld arc power (current x closed circuit voltage), v is the weld arc advance rate, A is the deposited weld metal cross-section area and N is the number of passes. This formula can be derived by assuming that the electrical heat input per unit mass of weld filler wire required to make a sound weld is invariant. A number of weld bead trials using 2.4, 3.2, 4 and 5mm diameter electrodes and different electrical power conditions were carried out to confirm the validity of this assumption and obtain the constant of proportionality. The expression should be used with caution for values of Q above about 1.8 KJ/mm.

The pipe welds examined cover a wide range of thickness (16 - 65mm), R/t ratio (2.8 - 25), weld heat input (1.0 - 2.4 KJ/mm) and heat input per unit thickness (15 - 136 KJ/mm^2). Residual stress measurements were performed using diverse techniques including neutron diffraction (ND), deep hole drilling (DH), surface centre-hole drilling (SH) and block removal splitting and layering (BRSL). A description of the techniques is beyond the scope of this paper. Some of the measurements are new, but many have been published recently (Bate et al., 2000), (Edwards et al., 1998), (Edwards et al., 2000), (Hutchings et al., 2000), (Smith et al., 2000).

The measured through-wall residual stress profiles are shown in Figs. 3 to 7. They include stresses through the weld centre-line (CL) and in the heat affected zone (HAZ). The line of the latter measurements is usually at the edge of the weld cap, or 1-3 mm from the edge (beneath cap). For the SP19 weld, measurements were made on both sides of the weld cap. The measurements are differentiated by being associated with the first cap pass (FCP) or last cap pass (LCP).

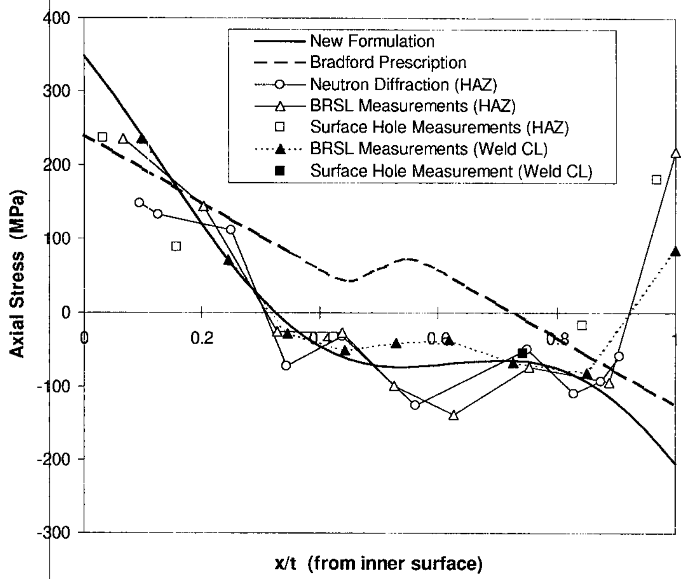

Figure 3: Axial residual stress measurements on Weld C, a type 316L stainless steel double-V prep. pipe girth weld (t=15.9mm, R/t=25, Q=2.2 KJ/mm, $\tilde{Q}$ =136 KJ/mm^2)

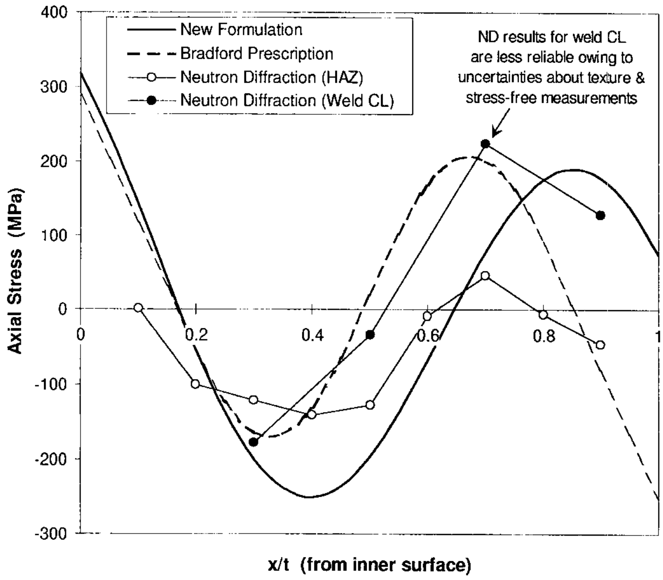

Figure 4: Axial residual stress measurements on weld OU20, a type 316L stainless steel J-prep. pipe girth weld (t=20mm, R/t=3.8, Q=1.8KJ/mm, $\tilde{Q}$ =91 KJ/mm^2)

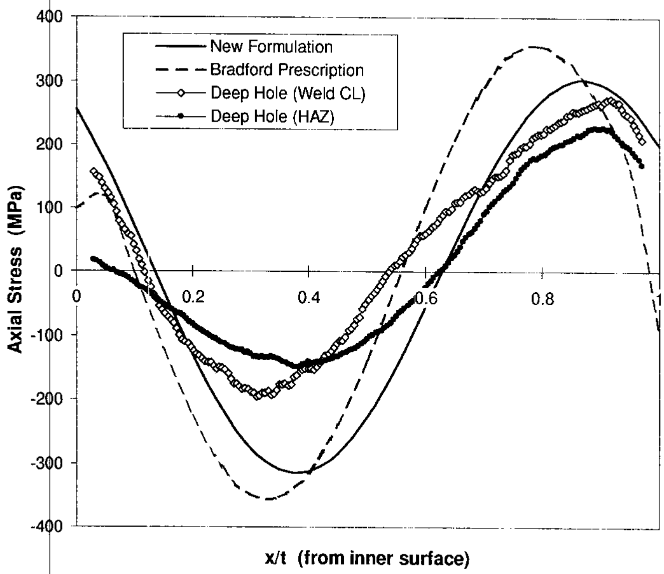

Figure 6: Axial residual stress measurements on weld SP37, a type 316H stainless steel J-prep. pipe girth weld (t=37mm, R/t=5.3, Q=2.2 KJ/mm, $\tilde{Q}$ =59 KJ/mm^2)

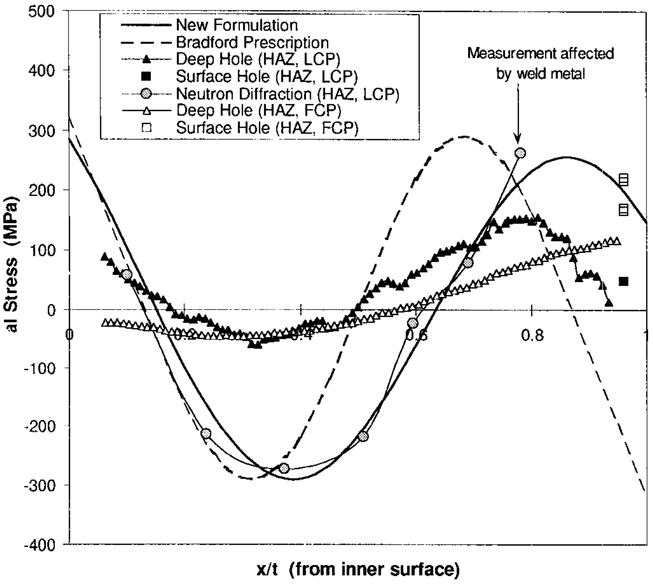

Figure 5: Axial residual stress measurements on weld SP19, a type 316H stainless steel J-prep. pipe girth weld (t=19.6mm, R/t=10.5, Q=1.4 KJ/mm, $\tilde{Q}$ =73 KJ/mm^2)

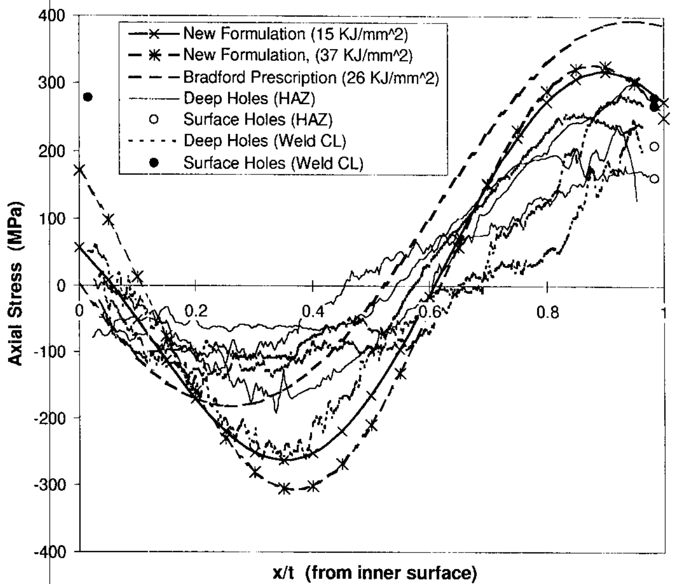

Figure 7: Axial residual stress measurements on weld S5, a type 316H stainless steel J-prep. pipe girth weld (t=65mm, R/t=2.8, Q=1.0-2.4 KJ/mm, $\tilde{Q}$ =15-37 KJ/mm^2)

In general, the stresses from different measurement methods for each weld type show good agreement with each other. Differences in stress profile associated with position in the weld or HAZ are evident, for example see Fig. 5. Here it should be noted that the DH measurements on SP19 were unable to fully resolve the stress gradients (as the DH method is better suited to thicker structures). This is particular true for the FCP measurement that used a larger 20mm diameter core size, whereas the LCP measurement used a 10mm diameter core that more successfully captured the stress profile. The HAZ neutron diffraction results for SP19 are slightly different to those reported by Edwards et al. (2000), following the availability of more accurate stress-free reference measurements. However, the ND stress measurements at the weld centre-line of OU20 should be interpreted with caution owing to uncertainties about texture and stress-free reference measurements for the weld material. Some of the scatter in Fig. 7 can be attributed to the range of weld heat inputs used.

A best estimate measured residual stress profile for the HAZ-LCP in SP19 is included in Fig.1 for comparison purposes. An equivalent profile for the HAZ-FCP for the outer 40% of the section thickness is also shown.

NEW RESIDUAL STRESS FORMULATION

The pipe measurements are compared with the Bradford profiles in Figs. 3-7, as these are the only ones available that attempt to characterise the weld detailed stress distribution. The maximum tensile stresses predicted by Bradford are consistent with measurements. The Bradford shape-fits to measurements are reasonably accurate except towards the outer surface (Figs. 3-6) and at weld root of the 65mm thick pipe (Fig. 7). In the case of the ..mm weld (Fig. 3), the measurements indicate the presence of a sharp outer surface gradient that is not conservatively modelled (from a fracture assessment viewpoint). The Bradford profile towards the outer surface of SP19 weld (Fig. 5) is also not quite right, and again non-conservative. For this weld, the measurements indicate the importance of weld pass sequence effects, as observed in finite element simulations (Edwards et al., 2000). The HAZ-FCP and HAZ-LCP have distinctly different profiles associated with either the first or last capping passes.

The Bradford residual stress prescription was developed to provide a good, generally bounding, representation of finite element profiles for a wide range of pipe geometries and weld heat inputs. This paper demonstrates that it is the best currently available for austenitic pipe girth welds. However, the profiles are not always self-equilibrating across the thickness and do not always capture tensile stresses towards the outer surface and at the weld root. The prescription is also not simple to apply as it requires interpolation of three tabulated parameters for a given weld pass heat input per unit thickness, $\tilde{Q}$.

A new formulation for axial stress distributions in stainless steel e girth welds is proposed that is more accurate compared with measurements, gives self-equilibrating profiles and is very simple to evaluate. The formulation uses a sine function (similar to Bradford) and includes an added linear component, following observations of (Dong et al., 2000).

$$\sigma_{axial}\left(\frac{x}{t}\right) = \sigma_y\left\{\beta\left(1-2\frac{x}{t}\right)+\alpha\sin\left[\frac{\pi}{4}+2\pi\left(1-\frac{x}{t}\right)\right]\right\} \quad (3)$$

where

$\frac{x}{t}$ = fractional distance through thickness from bore

$\sigma_y = \mathrm{Max}(\sigma_{weld1\%PS}, \sigma_{parent\,10\%PS})$

$$\alpha = -8.89\times10^{-5}\tilde{Q}^2 + 1.10\times10^{-2}\tilde{Q} + 0.359 \quad (4)$$

$$\beta = 6.74\times10^{-3}\tilde{Q} - 0.339 \quad (5)$$

for 15 KJ/mm^2 < $\tilde{Q}$ < 150 KJ/mm^2

The above model is physically reasonable as the first part of the equation represents a through-wall bending component of stress (tension at inner surface) induced by the tourniquet contraction of the weld metal. This deformation response tends to be dominant for thinner walled pipes with high heat input welding parameters ($\tilde{Q}$ > 120 KJ/mm^2). In thicker section pipes, sequentially deposited weld beads incrementally compress underlying passes leading to a more complex, self-balancing distribution across the thickness. A bounding sinusoid profile has been chosen that generally gives a tensile stress at the weld root (that is invariably observed) and high tensile stress near the outer surface (to cover capping bead effects). Note that for lower heat inputs per unit thickness ($\tilde{Q}$ < 50 KJ/mm^2), the through-wall bending component becomes reversed (tension on outer surface).

The profiles predicted by this formulation are compared with the pipe weld residual stress measurements in Figs. 3-7. It is evident that the new profiles provide a slightly better general correlation with measurements than the Bradford prescription. The outer surface 'skin' effect in the 16mm weld (Fig. 3) is the only anomaly.

DISCUSSION

The accuracy of most of the recommended axial residual stress profiles for the 19.6mm thickness weld, SP19, is poor compared with measurements (Fig. 1). Some are evidently conservative for fracture assessment purposes, but the degree of conservatism depends on the size and location of defect considered. The linear through-wall bending distributions are non-conservative for the outer surface defect considered. The Bradford profile is the only one that gives a reasonable estimate of the detailed stress distribution (Fig. 5), although it does not conservatively bound stresses at the outer surface. The general findings for SP19 also apply to the other pipe welds considered in this paper (Figs. 3-4, 6-7), for which integrity assessment procedures and compendia also recommend widely different axial residual stress profiles.

The Bradford prescription was based on finite element model results for the residual stress field. It is therefore of some interest that it generally provides a reasonable description of the <u>measured</u> residual stresses. This provides indirect evidence validating the finite element results employed by Bradford against the measurements.

The new formulation presented in this paper has improved on the Bradford prescription derived from finite element results. It provides the most accurate and generally conservative detailed description of measured axial residual stresses in the stainless steel pipe girth welds examined. It is simple to evaluate and gives profiles that are self-equilibrating (zero mean stress) through the section. Following Bradford, the formulation recognises the central role of strain hardening in the creation of the weld and HAZ residual stresses by defining the amplitude of the stress distribution through the greater of the parent 10% proof stress properties and the weld 1% proof stress. This is unusual as previous recommended profiles, for example (BSi, 2000) and (SINTAP, 1999), have employed the parent 0.2% or 1% proof stress.

The new formulation discriminates between a through-wall bending component of residual stress and self-equilibrating oscillations. Thus the new profiles capture both the underlying stress distribution controlling ultimate failure and also the detailed local stress field. This enables easy classification of the former component as medium-range, and the latter as short-range in R6 procedure assessments. By this means residual stresses are treated in the most effective way in fracture assessments.

The wide range of pipe thickness (16 - 65mm), R/t ratio (2.8 - 25) and weld heat input (1.0 - 2.4KJ/mm) considered in this paper gives high confidence in the validity of the new formulation, for MMA and SAW welds. Further comparisons are desirable for thin-wall ($t < 16mm$), small-diameter girth welds where residual stresses can be sensitive to the detailed welding procedure. For example Keim et al. (2000) report significant circumferential variations in axial residual stress associated with weld start and stop effects in a 114mm outer diameter, 6.3mm thick pipe weld.

This paper has not discussed weld hoop stresses, although these were also measured on the pipes examined. A comparison of the Bradford (2000) prescription for hoop stresses with measurements will be reported in a future publication.

CONCLUSIONS

1. Structural integrity assessment procedures and compendia recommend widely different through-wall axial residual stress profiles for pipe girth welds.
2. Fracture assessments for pipe girth welds containing defects under typical plant loading conditions are very sensitive to the assumed residual stress profile and magnitude.
3. The accuracy of most of the recommended profiles is poor, compared with residual measurements on a wide range of pipe girth welds.
4. The prescription of Bradford (2000), based solely on finite element results, provides a reasonably accurate and detailed description of measured axial through-wall residual stresses in pipe girth welds, but does not always capture tensile stresses towards the outer surface and at the weld root, or weld pass sequence effects in thinner pipe welds.
5. A new formulation is presented that improves on Bradford's prescription and provides the most accurate and generally conservative detailed through-wall profile of measured axial residual stresses in the stainless steel pipe girth welds examined. The new approximation is simple to evaluate and gives stress distributions that are self-equilibrating through the section. It is therefore ideally suited for use in fracture assessments.
6. The new formulation is valid for MMA and SAW stainless steel girth welds having a wall thickness in the range 16 to 65mm, R/t ratio between 2.8 and 25, weld heat input in the range 1.0 to 2.4KJ/mm and heat input per unit thickness of between 15 and 150 KJ/mm^2.

ACNOWLEDGEMENT

This paper is published with the permission of British Energy Generation Ltd.

REFERENCES

American Petroleum Institute (API), 2000, "API Recommended Practice 579", First Edition, American Petroleum Institute, Washington.

American Society of Mechanical Engineers (ASME), 1986, Section XI Task Group for Piping Flaw Evaluation, ASME Code, "Evaluation of Flaws in Austenitic Steel Piping", J. Pres. Ves. Technology, Vol. 108, pp. 352-366.

Bate S. K., 2000, "Compendium of Residual Stress Profiles for R6", AEA Technology Report AEAT/NJCB/000006/00.

Bate S. K., Bouchard P. J., Flewitt P. E. J., George D., Leggatt R. H., Youtsos A. G., 2000, "Measurement and Modelling of Residual Stresses in Thick Section Type 316 Stainless Steel Welds", Proc. ICRS-6, IOM Communications Ltd., pp. 1511-1518.

Bradford R. A. W., 2000, "Through-thickness Distributions of Welding Residual Stresses in Austenitic Stainless Steel Cylindrical Butt Welds", Proc. ICRS-6, IOM Communications Ltd., pp. 1373-1381.

Brickstad B., Josefson L., 1998, "A Parametric Study of Residual Stresses in Multi-pass Butt-Welded Stainless Steel Pipes", Int. J. Press. Ves. & Piping, 75, pp 11-25.

British Energy, 2000, "Assessment of the Integrity of Structures Containing Defects", British Energy Generation Ltd. Procedure R6 Revision 3.

British Energy, 2001, "Assessment of the Integrity of Structures Containing Defects", British Energy Generation Ltd. Procedure R6 Revision 4.

British Standards Institution (BSi), 2000, "Guide on Methods for Assessing the Acceptability of Flaws in Metallic Structures", BS7910:1999, Incorporating Amendment No. 1, London.

Dong, P., Osage, D., and Prager, M., 2000, "Development of Weld Residual Stress Distributions for Fitness for Service Assessment," ASME PVP-Vol. 411, Special Topics in Life Assessment, ASME PVP Conference, Seattle, Washington, pp. 53-64.

Edwards L., Bouchard P. J., Dutta M., Fitzpatrick M. E., 1998, "Direct Measurement of Residual Stresses at a Repair Weld in an Austenitic Steel Tube", Proc. Conf. on Integrity of High Temperature Welds, PEP Ltd., pp. 181-191.

Edwards L., Bruno G., Dutta M., Bouchard P. J., Abbott K. L., Lin Peng R., 2000, "Validation of Residual Stress Predictions for a 19mm Thick J-Preparation Stainless Steel Pipe Girth Weld using Neutron Diffraction", Proc. ICRS-6, IOM Communications Ltd., pp. 1519-26.

Hutchings M. T., Withers P. J., Bouchard P. J., 2000, "Characterisation of the Residual Stress State in a Double 'V' Stainless Steel Cylindrical Weldment using Neutron Diffraction and Finite Element Simulation", Proc. ICRS-6, IOM Communications Ltd., pp. 1333-1340.

Keim E., Weiss E., Fricke S., Schmidt J., 2000, "Effect of Last pass Heat Sink Welding and Service Transients on Residual Stresses", Proc. ICRS-6, IOM Communications Ltd., pp. 1433-1442.

SINTAP, 1999, 'Structural Integrity Assessment Procedures for European Industry', EC Contract BRPR-CT95-0024 Final Report, Brussels.

Smith D. J., Bouchard P. J., George D., J., 2000, "Measurement and Prediction of Residual Stresses in Thick Section Steel Welds", J. Strain Anal. 35, pp. 287-305.